

# AN EXPERIMENTAL INVESTIGATION INTO THE MECHANICAL BEHAVIOR OF 3D WOVEN HYBRID COMPOSITES

\* Rajesh Mishra  
B. P. Dash  
B. K. Behera

Indian Institute of Technology Delhi  
Department of Textile Technology  
India

\* [rajesh.mishra@gmail.com](mailto:rajesh.mishra@gmail.com)

## Abstract

In general, the purpose of hybridization is to achieve a composite architecture which synergizes the properties of both materials and/or lowers the cost since one of the fibers could be too expensive. In this study, 3D woven glass/aramid/epoxy hybrid composites were fabricated by using Kevlar and zylon in Z direction and glass in both X and Y direction. Their mechanical behavior such as tensile, compression, 3 point bending, impact resistance, stab resistance and DMA has been investigated. 3D hybrid composites clearly show better impact resistance, stab resistance and DMA properties as compared to neat composite of comparable FVF.

## Introduction

It has been revealed that 3D woven composites have distinct mechanical and physical properties compared with their 2D laminated counterparts [1, 2]. They cost reasonably due to their relatively simple resin impregnation process [3] and better performance because of their resistance to delamination [4, 5]. In addition, 3D composites have good ballistic impact damage resistance and significantly high low velocity impact tolerance [6–8]. Low velocity impact properties of 3D woven composites are important for their various applications. This type of loading can occur when tools are dropped on the surface of a composite or when the material is impacted by debris, fragments, or projectiles. Hybrid composites contain two or more different types of reinforcement fibers which have different mechanical and/or other properties, allowing researchers to design a composite with tailored properties in specific applications [9–11]. In general, the purpose of hybridization is to achieve a composite architecture which synergizes the properties of both materials and/or lowers the cost since one of the fibers could be too expensive. Structures of hybrid composites may be classified as interply hybrids, intraply hybrids, intimately mixed (intermingled) hybrids, selective placement and super hybrid composites [12]. Brittle inorganic fibers and ductile organic fibers are often combined to make hybrid composites such as palm/glass, glass/mineral fiber, aramid/glass, etc. [13–15]. The so-called hybrid effect often occurs in the form of a positive deviation of a certain property from the ‘rule of mixtures’ [16].

Mechanical properties including low velocity impact properties of a hybrid composite have not been studied extensively. Among limited publications in this subject area, Pegoretti and co-workers [12] studied low velocity impact behavior of E-glass/PVA hybrid laminated woven composites in two structures, namely interply and intraply hybrids. In that research, the intraply composites were composed of fabric layers, in which the warp yarns and the weft yarns were different types. It was found that the intraply hybrid composites had better tensile and impact performance than their interplay counterparts. Impact properties of 3D woven composites have been studied [3, 17–20]. However, little has been reported regarding the

mechanical behavior of hybrid 3D woven composites, in particular varying through the thickness direction fiber. As an inorganic fiber, glass fibers are widely used in textile composites due to relatively low cost and good performance. They have a very good tensile strength. Especially if they are made thinner, the strength per unit cross section becomes greater. Glass fiber is stronger than the steel wire of the same thickness. It has break elongation is 3.5-4 percent.

Aramid fibers, on the other hand, have good tensile strength and modulus as well as superior impact resistance, though they are much more expensive than glass fibers. Therefore a 3D woven hybrid composite of these two fibers will be reasonably priced with reasonable tensile, compression and impact properties. However, it is not clear how the impact properties of the hybrid composites will be changed when the construction of the 3D woven changes. In this study, 3D woven glass/aramid/epoxy hybrid composites were fabricated by using Kevlar and zylon in Z direction and glass in both X and Y direction.

## 1 Development of 3D woven hybrid fabrics in 2D weaving system using various

### 1.1 Fabric construction parameters

The neat fabric was prepared from multifilament 600 Tex E-glass tow in rigid rapier weaving machine. Kevlar and Zylon tows of 666 tex and 650 tex were used as binder for hybrid fabrics. The stuffer and filler tows remained 600 tex E-glass. Modifications were made for mounting an extra beam to supply binder warp in existing 2D weaving system. Constructional details of each fabric are laid down below in Table 1.

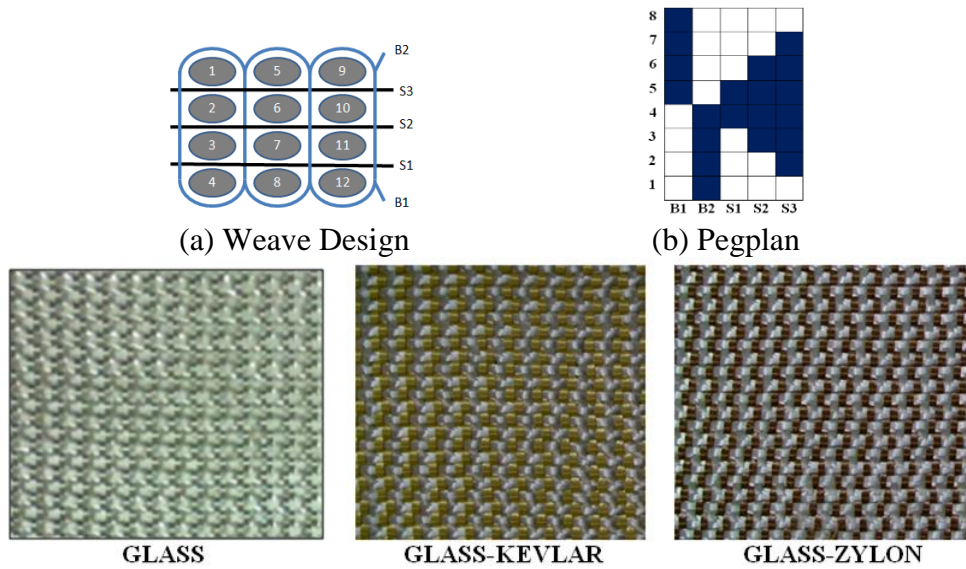
*Tab. 1: Construction parameters of different fabric*

|                                      | 3D Orthogonal<br>Glass | 3D Orthogonal<br>Glass-Kevlar | 3D Angle Orthogonal<br>Glass-Zylon |
|--------------------------------------|------------------------|-------------------------------|------------------------------------|
| <b>Reed count</b>                    | 24                     | 24                            | 24                                 |
| <b>Stuffer or warp ends /<br/>mt</b> | 158                    | 158                           | 158                                |
| <b>Binder ends /mt</b>               | 315                    | 315                           | 315                                |
| <b>Fabric width in mt</b>            | 0.41                   | 0.41                          | 0.41                               |
| <b>Picks / mt</b>                    | 315                    | 315                           | 315                                |

*Source: Own*

#### 1.1.1 Weave design of fabrics

Weave design and peg plan and images of 3D neat glass and hybrid fabric samples are given in Fig. 1.



Source: Own

**Fig. 1:** Weave design, Pegplan and Images of 3D neat glass and hybrid fabrics

## 1.2 Fabric dimensional parameters

Measured values of fabric dimensional parameters are given in Table 2.

**Tab. 2:** Measured parameters of fabric samples

| Fabric type                        | 3D Orthogonal Glass | 3D Orthogonal Glass-Kevlar | 3D Angle Orthogonal Glass-Zylon |
|------------------------------------|---------------------|----------------------------|---------------------------------|
| Thickness (mm)                     | 1.4                 | 1.65                       | 1.62                            |
| Areal Density (Kg/m <sup>2</sup> ) | 1.248               | 1.278                      | 1.272                           |
| FVF of fabric                      | 0.35                | 0.35                       | 0.34                            |

Source: Own

## 2 Experimental Design for optimization of process parameters for composite manufacture

When multiple variables are involved, it becomes difficult to study the system using the common approach of varying only one factor at a time, while holding the others constant. A more efficient way to investigate these systems is to develop a mathematical model describing the relationship between the response and independent variables, in which the significance of individual factors and multifactor interactions can be determined [21-24]. A Box-Behnken Design (BBD) is a versatile method to statistically model and optimizes response variables that are affected by multiple independent factors. Statistical analysis, modeling, and numerical optimization were performed using Design Expert software, Design-Expert 8.0.7.1. The BBD matrix generated by Design Expert software displays factor levels in the experimental design in two ways: (i) the actual factor levels, which are the values from the experiment, and (ii) the coded factor levels, +1, -1, and 0, for high levels, low levels, and center point, respectively. The BBD experimental design matrix is shown in terms of both actual and coded factor levels in Table 3. Twelve replicates were run for each experiment along with one center point.

**Tab. 3:** Box-Behnken design matrix in terms of both actual and coded factor levels generated by design expert software

| Run | Factor 1<br>Add on % | Factor 2<br>Hardner % | Factor3<br>Pressure (Bar) | Response 1<br>Total Energy<br>(Joule) | Response 2<br>Peak Force<br>(Newton) |
|-----|----------------------|-----------------------|---------------------------|---------------------------------------|--------------------------------------|
| 1   | -1(45)               | 0(12)                 | 1(12)                     | 12.6                                  | 2597                                 |
| 2   | 0(50)                | -1(10)                | 1(12)                     | 12.7                                  | 2824                                 |
| 3   | 0(50)                | 0(12)                 | 0(10)                     | 11.5                                  | 2553                                 |
| 4   | 1(55)                | 1(14)                 | 0(10)                     | 8.5                                   | 1887                                 |
| 5   | 0(50)                | 1(14)                 | -1(8)                     | 9.7                                   | 2353                                 |
| 6   | 1(55)                | 0(12)                 | -1(8)                     | 9.0                                   | 1998                                 |
| 7   | 0(50)                | 1(14)                 | 1(12)                     | 10.5                                  | 2331                                 |
| 8   | 1(55)                | 0(12)                 | 1(12)                     | 9.4                                   | 2098                                 |
| 9   | -1(45)               | 1(14)                 | 0(10)                     | 11.5                                  | 2553                                 |
| 10  | -1(45)               | 0(12)                 | -1(8)                     | 10.4                                  | 2309                                 |
| 11  | -1(45)               | -1(10)                | 0(10)                     | 11.0                                  | 2442                                 |
| 12  | 1(55)                | -1(10)                | 0(10)                     | 11.2                                  | 2514                                 |
| 13  | 0(50)                | -1(10)                | -1(8)                     | 10.9                                  | 2420                                 |

Source: Own

## 2.1 Statistical Analysis of the Model

For both total energy and peak force, regression analysis of the experimental data showed that in terms of coded factors, these were described as:

$$Total\ energy = 11.5 - 0.94 * add\ on - 0.68 * hardner + 0.65 * pressure - 0.75 * add\ on * hardner - 0.44 * add\ on * hardner * pressure - 0.8 * add\ on^2 - 0.19 * hardner^2 + 0.34 * pressure^2 \quad (1)$$

and

$$Peak\ force = 2553 - 175.5 * add\ on - 134.5 * hardner + 96.1 * curing\ pressure - 184.5 * add\ on * hardner - 47 * add\ on * curing\ pressure - 106.5 * hardner * pressure - 217 * add\ on^2 + 13.9 * hardner^2 - 84.7 * pressure^2 \quad (2)$$

For total energy all three parameters along with interaction between add on and hardner were found to be significant since their corresponding F values are less than 0.05. Similarly for peak force, along with the previously stated factors interaction between hardner % and pressure and square of add on were found to be significant.

**Tab. 4:** ANOVA for Response Surface Quadratic Model (Total Energy)

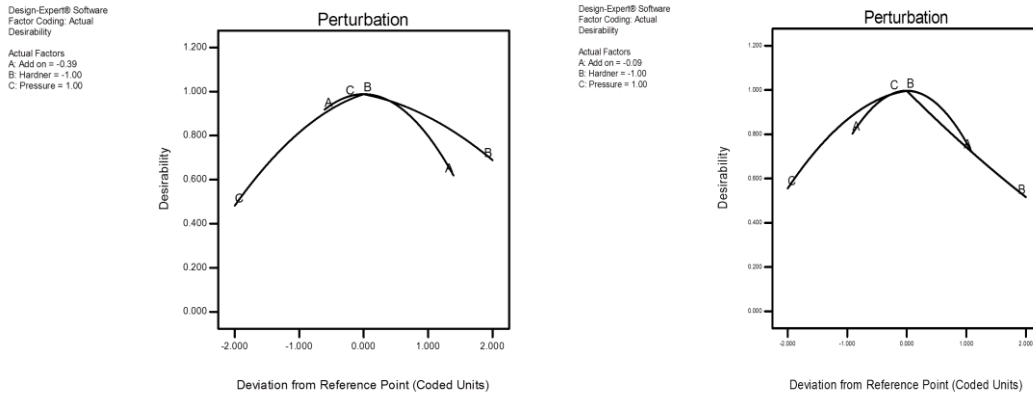
| Analysis of variance table [Partial sum of squares - Type III] |          |    |          |          |          |             |
|--|----------|----|----------|----------|----------|-------------|
|  | Sum of   |    | Mean     | F        | p-value  |             |
| Source   | Squares  | df | Square   | Value    | Prob > F |             |
| Model  | 19.0731  | 9  | 2.119233 | 11.10284 | 0.0363   | significant |
| A-Add on   | 7.125313 | 1  | 7.125313 | 37.33012 | 0.0088   | significant |
| B-Hardner  | 3.745585 | 1  | 3.745585 | 19.62344 | 0.0214   | significant |
| C-Pressure   | 3.411272 | 1  | 3.411272 | 17.87195 | 0.0242   | significant |
| AB   | 2.25     | 1  | 2.25     | 11.78794 | 0.0414   | significant |
| AC   | 0.765625 | 1  | 0.765625 | 4.011175 | 0.1389   |             |
| BC   | 0.237169 | 1  | 0.237169 | 1.242549 | 0.3462   |             |
| A <sup>2</sup>   | 1.473849 | 1  | 1.473849 | 7.721622 | 0.0491   | significant |
| B <sup>2</sup>   | 0.088706 | 1  | 0.088706 | 0.46474  | 0.5443   |             |
| C <sup>2</sup>   | 0.255749 | 1  | 0.255749 | 1.339892 | 0.3308   |             |
| Residual   | 0.572619 | 3  | 0.190873 |          |          |             |
| Cor. Total   | 19.64572 | 12 |          |          |          |             |

Source: Own

**Tab. 5:** ANOVA for Response Surface Quadratic Model (Peak Force)

| Analysis of variance table [Partial sum of squares - Type III] |          |    |          |          |          |             |
|--|----------|----|----------|----------|----------|-------------|
|  | Sum of   |    | Mean     | F        | p-value  |             |
| Source   | Squares  | df | Square   | Value    | Prob > F |             |
| Model  | 797951.9 | 9  | 88661.32 | 43.89245 | 0.0050   | significant |
| A-Add on   | 246254.6 | 1  | 246254.6 | 121.9102 | 0.0016   | significant |
| B-Hardner  | 144802.7 | 1  | 144802.7 | 71.68567 | 0.0035   | significant |
| C-Pressure   | 73935.51 | 1  | 73935.51 | 36.60233 | 0.0091   | significant |
| AB   | 136161   | 1  | 136161   | 67.40752 | 0.0038   | significant |
| AC   | 8834.12  | 1  | 8834.12  | 4.373397 | 0.1276   |             |
| BC   | 45390.3  | 1  | 45390.3  | 22.47081 | 0.0178   | significant |
| A <sup>2</sup>   | 108591.4 | 1  | 108591.4 | 53.75899 | 0.0052   | significant |
| B <sup>2</sup>   | 445.7628 | 1  | 445.7628 | 0.220678 | 0.6706   |             |
| C <sup>2</sup>   | 16394.05 | 1  | 16394.05 | 8.115997 | 0.0652   |             |
| Residual   | 6059.902 | 3  | 2019.967 |          |          |             |
| Cor. Total   | 804011.8 | 12 |          |          |          |             |

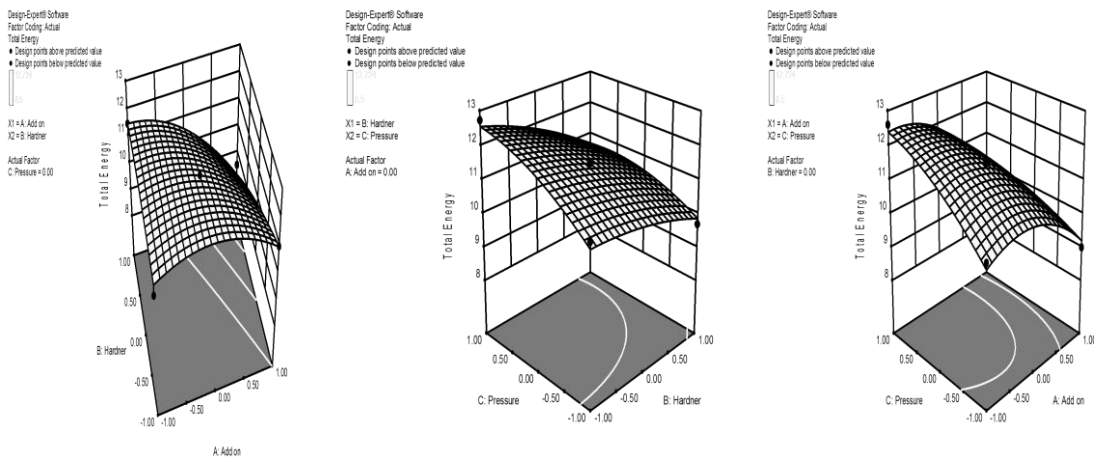
Source: Own



Source: Own

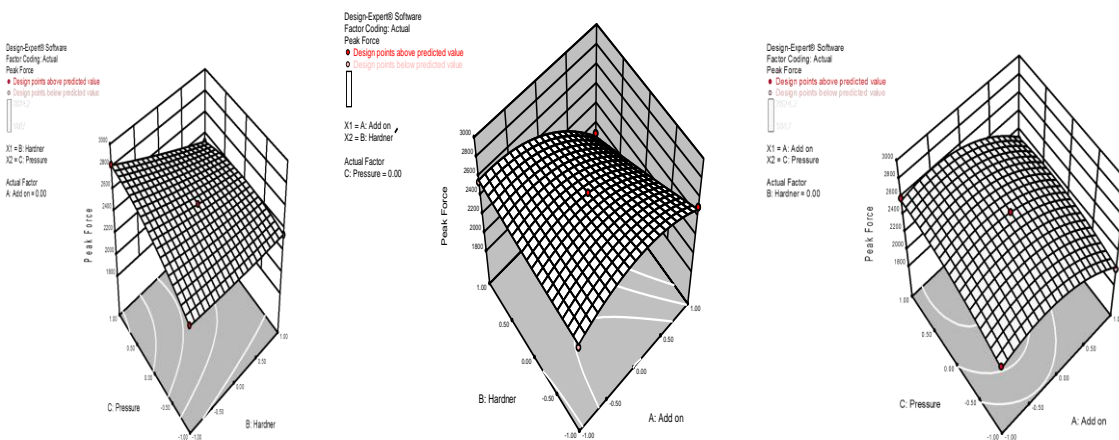
**Fig. 2:** Perturbation plots for total energy and peak force

The perturbation plots of the total energy and peak force against Add on, Hardner and curing pressure shown in Fig. 2 depicts the contribution of each factor. The perturbation plot illustrates the changes in total energy and peak force as each factor moves from the chosen reference with all other factors held constant at the middle level of the design space.



Source: Own

**Fig. 3:** 3D Surface plot showing effect of add on and hardner, hardner and curing pressure and add on and curing pressure on total energy



Source: Own

**Fig. 4:** 3D Surface plot showing effect of hardner and curing pressure, add on and hardner and add on and curing pressure on peak force

After observing both the perturbation plots and the 3D surface plots Fig.2, Fig.3 and Fig.4 it was concluded that 3D woven composite could be made with 48% add on, 10% hardner and 12 bar curing pressure to get highest total energy. Similarly for getting the highest peak force 49.55% add on, 10%hardner and 12 bar pressure should be maintained. Hence it was decided to manufacture 3D woven composites with 50%add on, 10% hardner and 12 bar curing pressure. All composites are prepared by compression moulding technique. LY556 Epoxy resin was used as a matrix component and it was applied by hand lay-up technique. The principal advantage of compression molding is its ability to produce parts of complex geometry in short periods of time. SANTECH compression moulding available in the workshop is used to prepare composites. The parameters set on the machine while preparing composites are mentioned below.

*Machine parameters maintained for composite manufacturing*

- Machine used :                    SANTECH compression moulding machine
- Curing time:                        900 sec.
- Breathing pressure:               6 bar
- Curing pressure:                   12 bar
- Curing temperature:               120 0c
- Hardener /Epoxy ratio:           1:10

**Tab. 6:** *FVF of different composites.*

| Type of reinforcement      | FVF   |
|----------------------------|-------|
| 3D Orthogonal Glass        | 39.6  |
| 3D Orthogonal Glass-Kevlar | 43.27 |
| 3D Orthogonal Glass-Zylon  | 42.21 |

*Source: Own*

### **3 Test methods for composite**

#### **3.1 Tensile Testing**

Tensile testing was performed with Instron 5582 using 50 KN load- cell according to ASTM 3039.The sample size was 250mm X 25mm, gauge length 150mm, cross head speed 2 mm/min. Ten readings were taken for each sample.

#### **3.2 Compression Testing**

Compression testing was performed with MTS 793 using 25 KN load- cell according to ASTM D3410.The sample size was 127mm X 25mm, gauge length 12.7 mm, cross head speed 1.5 mm / min. Ten readings were taken for each sample. This test method determines the in-plane compressive properties of polymer matrix composite materials reinforced by high-modulus fibers. In this test the compressive force into the specimen through shear at wedge grip interfaces. This type of force transfer differs from the procedure in test method D695 where compressive force is transmitted into the specimen by end-loading. The shear force was applied via wedge grips in a specially-designed fixture.

### **3.3 Flexural Testing**

Compression testing was performed with Zwick Z 010 using 1 KN load-cell according to ASTM D 790. The sample size was 120 mm X 12.7 mm, support span 50 mm, cross head speed 3 mm/min. Five readings were taken for each sample. All samples were tested in a control limit of 5% extension to measure the force required to bend the samples so that the modulus can be calculated. The span-to-depth ratio higher than 16:1 was chosen such that failure occurs in the outer fibers of the specimens and is due only to the bending moment eliminating shear effects.

### **3.4 Low velocity impact testing**

Impact test of all the composite structures was carried out to estimate the amount of impact energy absorbed by each composite. The tests were performed as per the ASTM D 7136. This test method determines the damage resistance of multidirectional polymer matrix composite laminated plates subjected to a drop-weight impact event. A flat, rectangular composite plate is subjected to an out-of-plane, concentrated impact using a drop-weight device with a hemispherical impactor. Sample size was 12 cm×12 cm, impactor speed – 5 m/min, and five reading were taken for each sample.

### **3.5 Knife penetration Test**

To carry out this test, the testomic tester M350-10CT was used. Each composite sample was placed on the plate of the machine. The machine head was dropped onto the sample thus holding the sample in place. The knife was then allowed to penetrate the fabric sample at a velocity of 1000 mm/min. A recording monitor was connected to this machine and it recorded the maximum force exerted on penetrating the sample. Five readings were taken for each composite sample.

### **3.6 DMA Test**

Dynamic Mechanical Analysis, otherwise known as DMA, is a technique where a small deformation is applied to a sample in a cyclic manner. This allows the materials response to stress, temperature, frequency and other values to be studied. Dynamic Mechanical Analysis (DMA) measures the mechanical properties of materials as function of temperature, frequency and time. It is a thermal analytical method by which the mechanical response of a sample subjected to a specific temperature program is investigated under periodic stress. Dynamic mechanical analyzer is a thermal analytical instrument used to test the mechanical properties of many different materials.

The storage modulus is measure of elasticity of material. It is also called “the ability of the material to store energy”. It is equivalent to the ability of a sample to store energy, i.e. its elasticity. Energy storage occurs as molecules are distorted from their equilibrium position by application of a stress. Removal of the stress results in a return to equilibrium position of the molecular segments.

Loss modulus represents the capability of a material to dissipate energy (mechanical, acoustic) as heat, owing to viscous motions inside the material itself. It is limited to the molecular motion within the sample that dissipates energy as heat.

Tan Delta ( $\delta$ ) is measure of material damping, such as vibration or sound damping. Damping refers to damping the loss of mechanical energy as the amplitude of motion gradually decreases. It also means the ability of a material to dissipate mechanical energy by converting it into heat. Tan Delta is a useful index of material viscoelasticity since it is a ratio of viscous

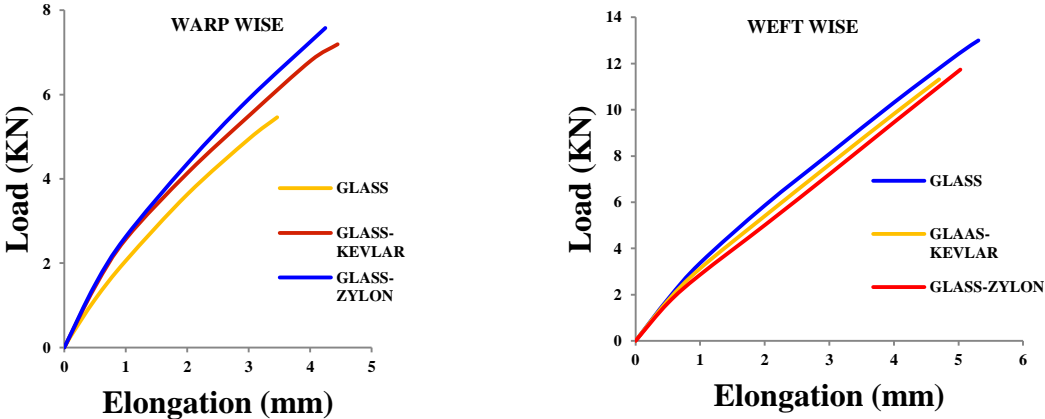
and elastic moduli.  $\tan\delta$  is an important indication of viscoelasticity of materials, it is independent from the shape and dimension of samples and it is dimensionless.

$$\tan \delta = \text{Loss Modulus} / \text{Storage Modulus} \tag{3}$$

Dynamic mechanical analysis was performed with DMA DX04T RMI instrument according to ASTM D 7028. The test was performed in three point bending mode with gauge length and sample width of 30 mm and 10 mm respectively. The samples were subjected to an oscillating frequency of 1 Hz and 100% oscillating amplitude in the temperature range 30 °C to 300 °C at the heating rate of 5 °C min<sup>-1</sup>. Five readings were taken for each sample. Storage Modulus and  $\tan\delta$  were generated as output.

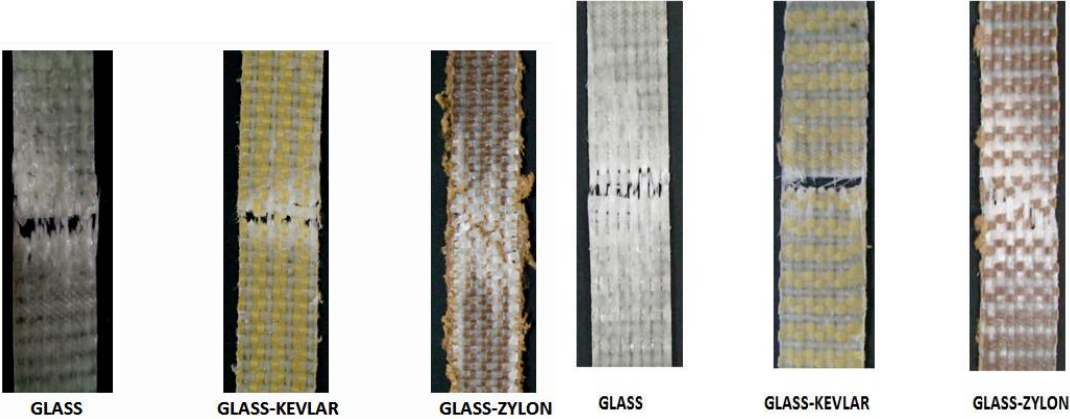
## 4 Results and Discussion

### 4.1 Tensile test



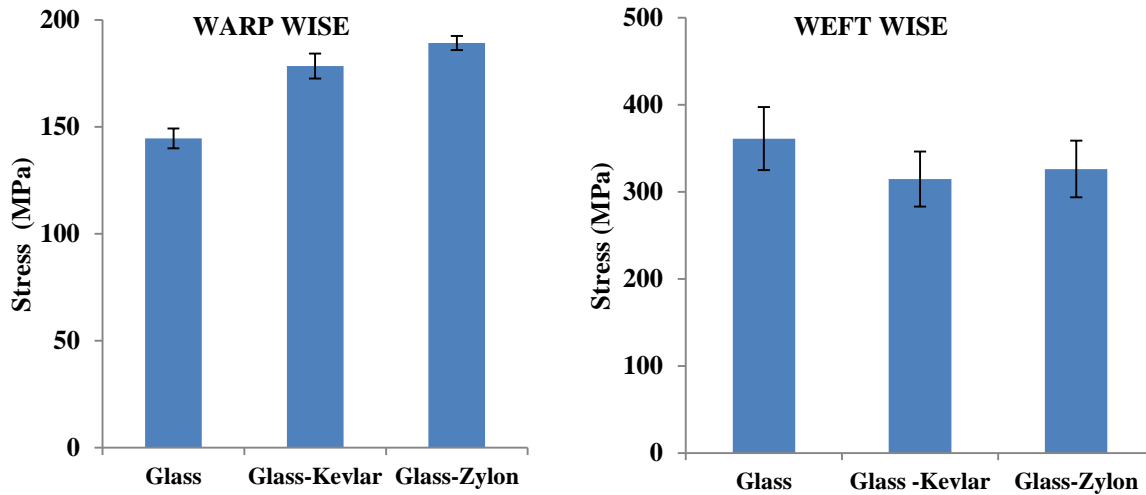
Source: Own

Fig. 5: Load elongation curve of different structures



Source: Own

Fig. 6: Images of hybrid composites after tensile testing



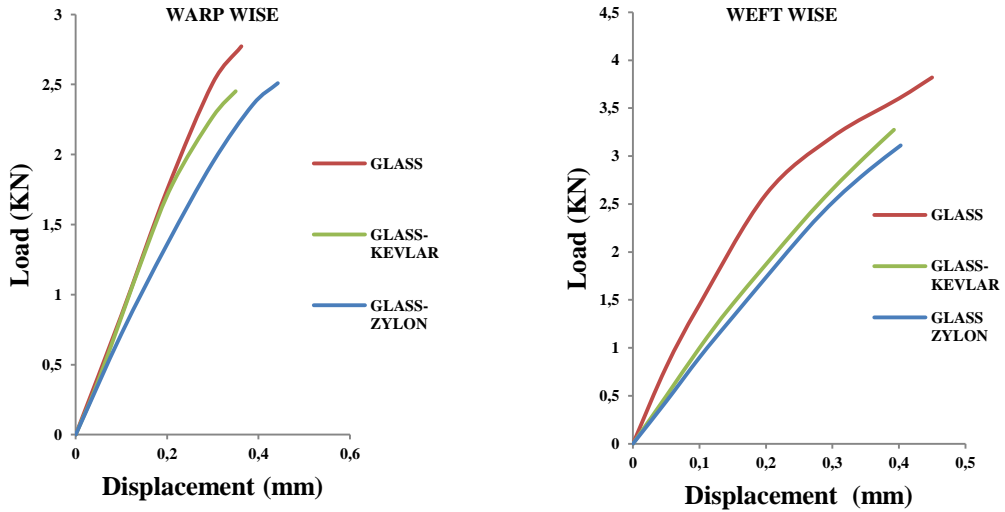
Source: Own

**Fig. 7:** Bar diagram for tensile stress of hybrid composites in both warp way and weft way

The typical load elongation curve generated from tensile test, the tested samples and the bar diagram depicting values of stress of different composites have been shown in Fig. 5, Fig. 6 and Fig. 7 respectively. Close observation into the tensile test results reveal that the ultimate load and stress increased 23% and 31% for glass-kevlar and glass-zylon hybridization. This improvement might have been due to the increase in fabric assistance values, due to the bulkier yarn structure of Kevlar and zylon. Moreover, during weaving the inter yarn friction between glass Kevlar and glass zylon was less resulting in less breakage of filaments. However, in weftwise direction the hybrid composites were found to have less strength than the neat glass composite, but this deviation is not significant. Moreover, from the images of tested samples it is observed that the damage area is less for the hybrid composites. This is evident by watching the opaque region surrounding the break.

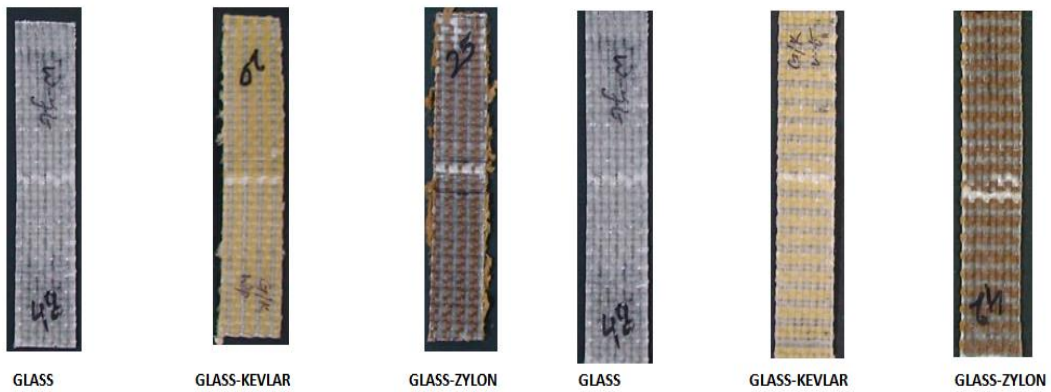
## 4.2 Compression Test

The typical load displacement curve generated from compressive test, the tested samples and the bar diagram depicting values of stress of different composites have been shown in Fig. 8, Fig. 9 and Fig. 10 respectively. Compressive properties of thin composite laminates are difficult to measure owing to sidewise buckling of specimens. A number of test methods and specimen designs have been developed to overcome the buckling problem. ASTM D 3410 method uses flat wedge grips instead of conical wedge grips. Flat wedge surfaces provide a better contact between the wedge and the tapered sleeve and improve the axial alignment to avoid the problem of buckling. Flat wedge grips can also accommodate variation in specimen thickness. Investigation into the compressive breaking stress of the composites reveals that the hybrid composites do exhibit poor strength when compared to the neat ones, in both warp way and weft way. But it was found that the warp way reduction was not significant while in weft way it is significant. This may be due to poor compressive properties of the Kevlar and zylon fiber accompanied by low interfacial bondage between these fibers and epoxy resin.



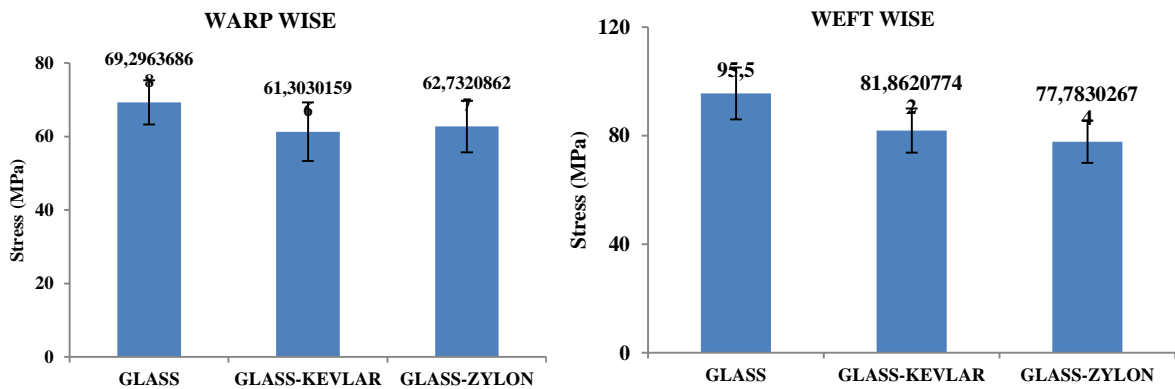
Source: Own

**Fig. 8:** Load elongation curve for compression test of hybrid composites in warp wise and weft wise direction



Source: Own

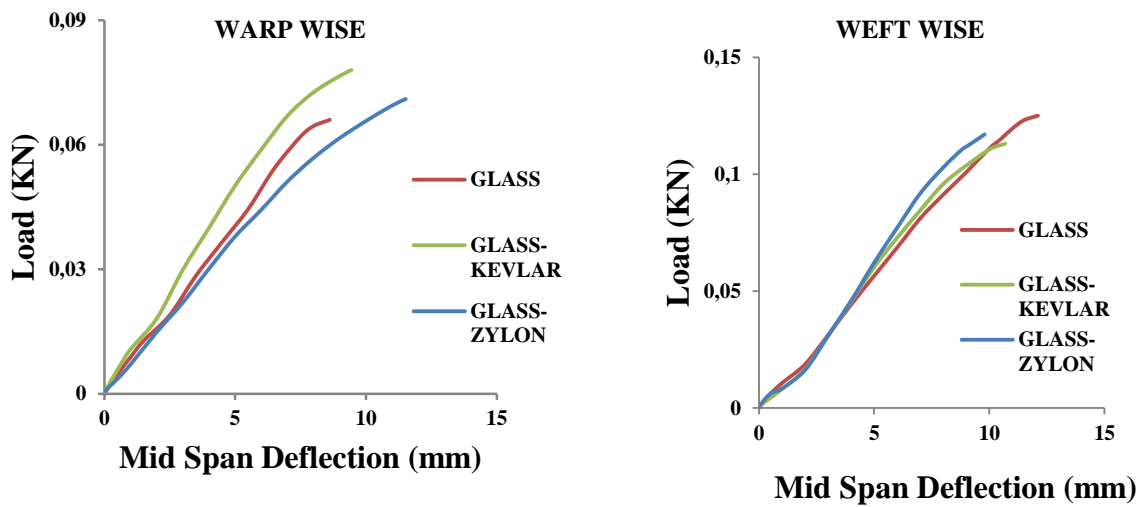
**Fig. 9:** Images of hybrid composites after compression test



Source: Own

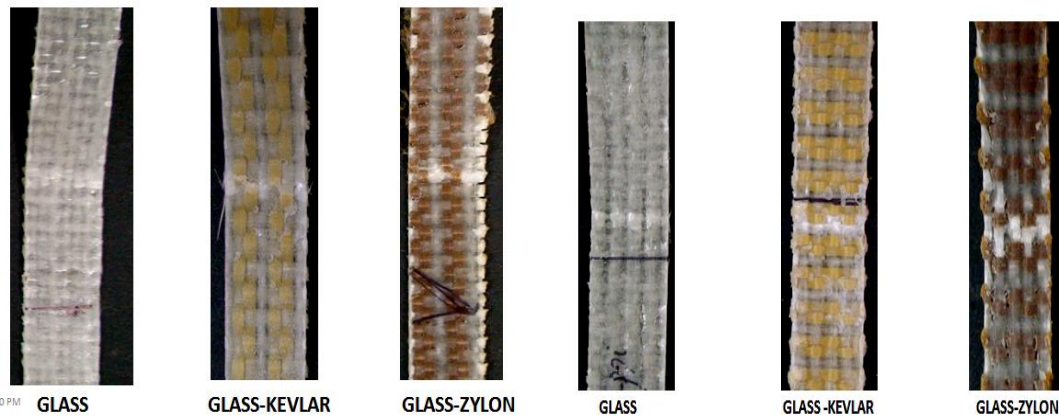
**Fig. 10:** Bar diagram for compressive stress of hybrid composites warp way and weft way

### 4.3 Three point bending test



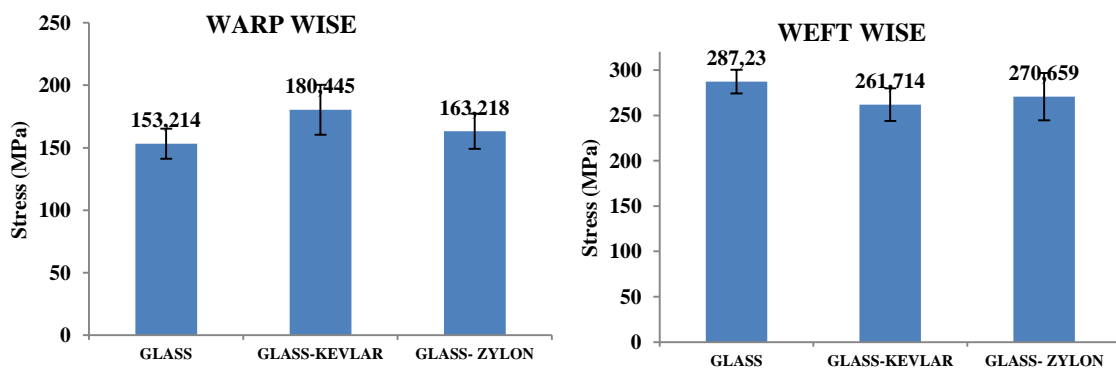
Source: Own

Fig. 11: Load deflection curve for 3 point bending of composites



Source: Own

Fig. 12: Images of composites after 3 point bending



Source: Own

Fig. 13: Bar diagram for 3 point bending stress and modulus of different structures in warp way and weft way

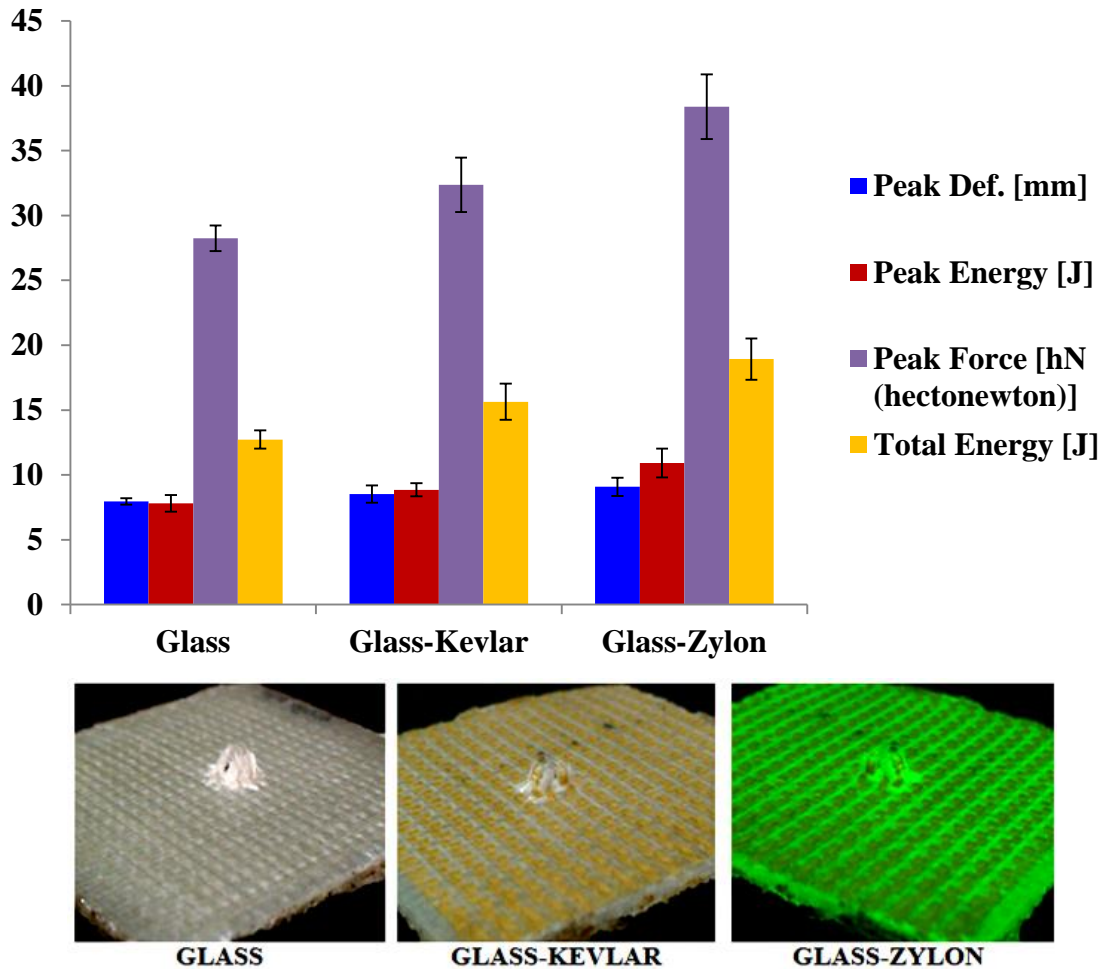
The load deflection curve generated from 3 point bending test, the tested samples and the bar diagram depicting values of stress of different composites have been shown in Fig. 11, Fig. 12 and Fig. 13 respectively. The failure of a composite during 3 point bending test is dependent

on three main factors: (1) the constituent materials, (2) the sequence in which the fibers are aligned and (3) the type of loading experienced in a specific direction. Common flexural loading failures include: compressive failure, tensile failure, shear and/or delamination. Delamination is the fracture along the direction of the fibre and is indicated by a laminate layer being separated from the composite. The other forms of failures will generally occur in the transverse direction because unidirectional composites are obviously anisotropic. The crack often initiates on the tension side of the beam and slowly propagates in an upward direction. Normally, the modulus is very sensitive to the matrix properties and matrix/fibre interfacial bonding. Tensile failures are not uncommon in flexural tests due to the fact that the outer layers undergo stretching. Should a composite fail in tension, it can be due to brittle failure or fibre pullout. Kinking is the most predominant form of compressive failure. However, composites might have also failed due to microbuckling, shear or splitting. Microbuckling of near surface stuffers does involve deflections out of the surface. In bending in-plane deflections of stuffers would have to occur in the weft direction and would therefore be strongly resisted by adjacent fillers [25-27].

Study of 3 point bending test results revealed that hybridization does not show up any particular trend on bending properties. However, almost 17% improvement in strength was observed in warp wise direction and 10% reduction in weft wise direction for glass Kevlar composite.

#### **4.4 Impact Test**

The bar diagram depicting values of peak deformation, peak energy, peak force and total energy absorbed by different composites and the impact tested samples have been shown in Fig. 14 and Fig. 15 respectively. The 3D hybrid composites clearly show better impact resistance compared to neat composites of comparable FVF. The glass zylon hybrid composite is found to absorb the highest amount of total energy, peak energy and peak force, followed by glass-kevlar and neat neat glass composite. Energy at peak is 39% and 13%, and total energy absorbed is 49% and 23 % higher for glass-zylon and glass-kevlar composites than the neat glass composites, due to incorporation of 15% yarn in Z direction. This may be due to the interlaminar toughening mechanisms, namely debonding, fracture, pull-out and, in particular, crack bridging of the z-binders impede the spread of delaminations from the impact site [28].

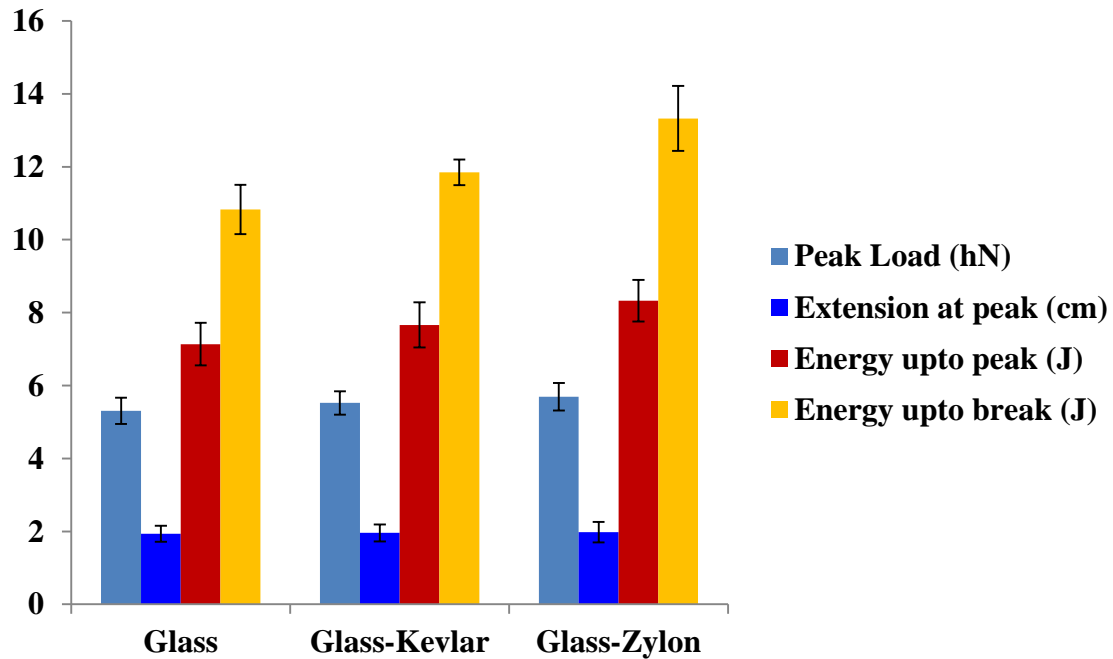


Source: Own

**Fig. 14:** Bar diagram for low velocity impact properties of composites

#### 4.5 Knife Penetration Test

Different test results of knife penetration test have been depicted in Fig. 16. 3D woven hybrid fabric reinforced composite shows better stab resistance compared to the neat composite. The 3D glass-zylon reinforced composite was observed to generate best stab resistance of all the samples tested. Energy up to peak and Energy up to break was found to be 8%, and 10% higher for glass-Kevlar than that of neat glass composite. Similarly for glass-zylon composite Energy up to peak and Energy up to break was found to be 95 and 23% higher than pure glass composite.



Source: Own

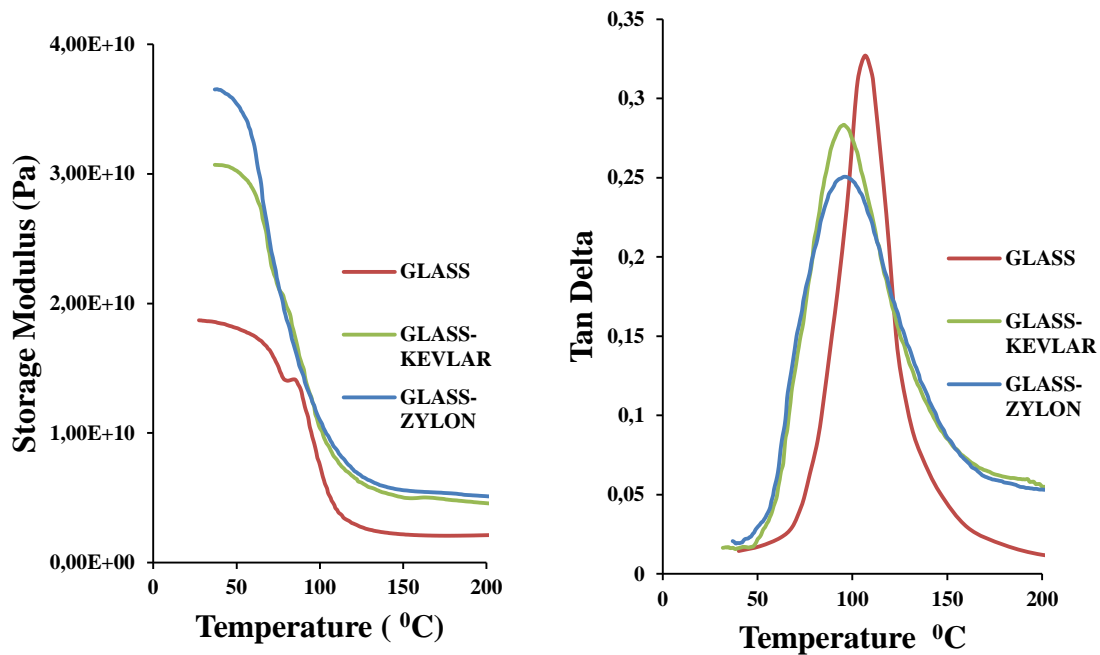
Fig. 15: Bar diagram for Knife penetration properties of composites

#### 4.6 DMA Test

The Dynamic Mechanical Analysis is a high precision technique for measuring the viscoelastic properties of materials. Viscoelasticity is about elastic behaviors of materials. Most real-world materials exhibit mechanical responses that are a mixture of viscous and elastic behavior. Dynamic Mechanical Analyzer (DMA) deforms a sample mechanically and after that it measures the sample response. When a force is applied on a material, it suffers a change in shape, i.e. it deforms. DMA measures stiffness and damping, these are reported as modulus and tan delta. The ratio of the loss modulus to the storage modulus is the tan delta and is often called damping. It is a measure of the energy dissipation of a material. Damping is the dissipation of energy in a material under cyclic load. It is a measure of how well a material can get rid of energy and is reported as the tangent of the phase angle. It is a parameter to measure how good a material will be at absorbing energy. It varies with the state of the material, its temperature, and with the frequency. Modulus values change with temperature and transitions in materials can be seen as changes in the tan delta curves. This includes not only the glass transition and the melt, but also other transitions that occur in the glassy or rubbery plateau. The glass transition ( $T_g$ ) is seen as a large drop in the storage modulus and a concurrent peak in the tan delta.

The study of storage modulus of composites reinforced with hybrid fabric, shown in Fig. 16 depict that the hybrid composites show higher values of storage modulus. When compared with the neat glass composite, 64% increase in storage modulus for glass-kevlar & 92% improvement for glass-zylon composites are observed, for almost similar FVF.

Observation of tan delta values in Fig. 17, with respect fiber hybridization reveal that the tan delta value is inversely proportional to the values of storage modulus i.e. it is highest for neat glass composite and lowest for glass-zylon composite. The  $T_g$  (Glass transition temperature), which is depicted by the picks of tan delta curve has occurred at 1060C for glass, 980 C for glass Kevlar and 950 C for glass zylon composites.



Source: Own

**Fig. 16:** Effect of temperature on storage modulus and tan delta of different composites

## Conclusion

It has been observed that warp wise tensile stress increase by 23% and 31% for glass-kevlar and glass-zylon hybridization. In weftwise direction the hybrid composites are found to have less strength than the neat glass composite, but this deviation is not significant. Hybrid composites do exhibit poor compressive strength compared to neat one; in both warp way and weft way. But it has been found that the warp way reduction is not significant, whereas in weft way it is significant. Study of 3 point bending test results has revealed that hybridization does not show up any particular trend on bending properties. However, almost 17% improvement in strength has been observed in warp wise direction and 10% reduction in weft wise direction for glass Kevlar composite. The 3D hybrid composites clearly shows better impact resistance compared to neat composite of comparable FVF. 3D woven hybrid fabric reinforced composites show better stab resistance compared to the neat composite. The 3D glass-zylon reinforced composite has been observed to generate best stab resistance of all the samples tested, hybrid composites show higher values of storage modulus. The tan delta value is inversely proportional to the values of storage modulus i.e. it is highest for neat glass composite and lowest for glass-zylon composite.

## Literature

- [1] BRANDT, J. et al.: Manufacture and performance of carbon/epoxy 3D woven composites. In: *Proceedings of the 37th international SAMPE symposium*, Anaheim, CA, 1992.
- [2] BRANDT, J; DRECHSLER, K.; ARENDTS, F. J.: Mechanical performance of composites based on various three-dimensional woven-fiber preforms. *Compos Sci Technol.* 1996; 56:381–6.
- [3] TAN, P et al.: *Compos: Part A* 2000; 31:259–71.
- [4] MOURITZ, A.P. et al.: Review of applications for advanced three dimensional fibre textile composites. *Compos: Part A* 1999; 30: 1445–61.

- [5] CHOU, T. W.; KO, F. K.: *Textile structural composites. Distributors for the U.S. and Canada*. Amsterdam (NY, USA): Elsevier Science; 1989.
- [6] MIRAVETE, A.: *3D textile reinforcements in composite materials*. Cambridge (UK): Woodhead Publishing Limited; 1999.
- [7] BAHEI-EL-DIN, Y. A.; ZIKRY, M. A.: Impact-induced deformation fields in 2D and 3D woven composites. *Compos Sci Technol*. 2003; 63:923–42.
- [8] CHOU, S; CHEN, H-C.; WU, C-C.: BMI resin composites reinforced with 3D carbon-fibre fabrics. *Compos Sci Technol*. 1992; 43:117–28.
- [9] ABDULLAH, Al K. et al.: Study on the mechanical properties of jute/glass fiber-reinforced unsaturated polyester hybrid composites: effect of surface modification by ultraviolet radiation. *J Reinf Plast Compos*. 2006; 25(6):575–88.
- [10] ANUAR H et al.: Tensile and impact properties of thermoplastic natural rubber reinforced short glass fiber and empty fruit bunch hybrid composites. *Polym Plast Tech. Eng*. 2006; 45:1059–63.
- [11] XIE, H.Q.; ZHANG, S.; XIE, D.: An efficient way to improve the mechanical properties of polypropylene/short glass fiber composites. *J Appl Polym Sci*. 2005; 96:1414–20.
- [12] PEGORETTI, A et al.: Intraply and interply hybrid composites based on E-glass and poly (vinyl alcohol) woven fabrics: tensile and impact properties. *Polym Int*. 2004; 53:1290–7.
- [13] HARIHARAN, A. B. A.; KHALIL, H.: Lignocellulose-based hybrid bilayer laminate composite: Part I – studies on tensile and impact behavior of oil palm fiber-glass fiber-reinforced epoxy resin. *J Compos Mater*. 2005; 39:663–84.
- [14] HARTIKAINEN, J et al.: Mechanical properties of polypropylene composites reinforced with glass fibres and mineral fillers. *Plast Rubber Compos*. 2004; 33:77–84.
- [15] IMIELINSKA, K.; GUILLAUMAT, L.: The effect of water immersion ageing on low-velocity impact behaviour of woven aramid-glass fibre/epoxy composites. *Compos Sci Technol*. 2004; 64:2271–8.
- [16] MAROM, G.; FISCHER, S.; TULER, F. R.; WAGNER, H. D.: Hybrid effects in composites – conditions for positive or negative effects versus rule-of-mixtures behavior. *J Mater Sci*. 1978; 13:1419–26.
- [17] KHALID, A. A.: The effect of testing temperature and volume fraction on impact energy of composites. *Mater Des*. 2006; 27:499–506.
- [18] BAUCOM, J.; ZIKRY, M.: Low-velocity impact damage progression in woven E-glass composite systems. *Compos: Part A* 2005; 36:658–64.
- [19] CHOU, S.; CHEN, H. C.; CHEN, H. E.: Effect of weave structure on mechanical fracture behavior of three-dimensional carbon fiber fabric reinforced epoxy resin composites. *Compos Sci Technol*. 1992; 45:23–35.
- [20] NAIK, N. K.; SEKHER, Y. C. et al.: Damage in woven-fabric composites subjected to low-velocity impact. *Compos Sci Technol*. 2000; 60:731–44.
- [21] MYERS, R. H.; MONTGOMERY, D. C. (1995), *Response Surface Methodology: Process and Product Optimization Using Designed Experiments*, Wiley, New York.

- [22] MATUANA, L. M.; LI, Q. (2004), Statistical Modeling and Response Surface Optimization of Extruded HDPE/Wood-Flour Composite Foams, *J. Thermoplast. Compos. Mater.* 17(2), 185-199.
- [23] MATUANA, L. M.; MENGELOGLU, F. (2002), Manufacture of rigid PVC/wood-flour composite foams using moisture contained in wood as foaming agent, *J. Vinyl & Addit. Technol.*, 8(4), 264-270.
- [24] MONTGOMERY, D. C. (2001), *Design and Analysis of Experiments*, 5th ed., Wiley, New York.
- [25] PIGGOTT, M. R.; HARRIS, B.: Compression strength of hybrid fibre-reinforced plastics. *J Mater Sci.* 1981; 16:687–93.
- [26] SUDARISMAN, D. I. J.: Flexural failure of unidirectional hybrid fibre-reinforced polymer (FRP) composites containing different grades of glass fibre. *Adv Mater Res.* 2008; 41–42:357–62.
- [27] DONG, C.; RANAWEERA-JAYAWARDENA, H. A.; DAVIES, I. J.: Flexural properties of hybrid composites reinforced by S-2 glass and T700S carbon fibres. *Composites: Part B* 2012; 43 573–581.
- [28] TONG, L; MOURITZ, A. P.; BANNISTER, M. K.: 3D Fibre Reinforced Polymer Composites, Elsevier Science Ltd 2002; ISBN 0-08-043938-1.

## EXPERIMENTÁLNÍ VÝZKUM MECHANICKÉHO CHOVÁNÍ 3D HYBRIDNÍCH KOMPOZIT

Obecně platí, že cílem hybridizace je dosáhnout kompozitní struktury, která posílí vlastnosti obou materiálů a / nebo sníží náklady, protože jeden typ vlákna může být příliš drahý. V této studii je popsána 3D tkanina sklo/aramid/epoxid hybridního kompozitu vyrobená z Kevlaru a Zylonu ve směru Z, a skla v obou směrech X a Y. Byly zkoumány mechanické vlastnosti, jako je pevnost v tahu, tlaku, třibodý ohyb, odolnost proti nárazu, odolnost proti propíchnutí a DMA. 3D hybridní kompozity ve srovnání s kompozitem FVF jasně ukazují lepší odolnost proti nárazu, odolnost proti probodnutí a vlastnosti DMA.

## EINE EXPERIMENTELLE UNTERSUCHUNG DES MECHANISCHEN VERHALTENS VON 3D-GEWOBENEN HYBRIDGEMISCHEN

Allgemein gilt, dass das Ziel der Hybridisierung im Erreichen einer gemischten Struktur ist, welche die Eigenschaften beider Materialien stärkt und/ oder die Kosten senkt, weil eine einzige Fasersorte zu teuer werden kann. In dieser Studie wird ein 3D-Gewebe aus Glas, Aramid und einem Epoxid eines hybriden Gemischs beschrieben. Dieses wird aus Kevlar und Zylon in Richtung Z und aus Glas in beiden Richtung X und Y hergestellt. Es wurden dessen mechanischen Eigenschaften wie Zugfestigkeit, Druck, Dreipunktbeweglichkeit, Stoßfestigkeit, Stichfestigkeit und DMA-Eigenschaften untersucht. 3D-Hybridgemische weisen im Vergleich mit dem Gemisch FVF eindeutig eine bessere Stoßfestigkeit, Stichfestigkeit und DMA-Eigenschaften auf.

## EKSPERYMENTALNE BADANIA MECHANICZNEGO ZACHOWANIA KOMPOZYTÓW HYBRYDOWYCH 3D

Ogólnie obowiązuje zasada, że celem hybrydyzacji jest osiągnięcie struktury kompozytowej, która poprawi właściwości obu materiałów i/lub zmniejszy koszty, ponieważ jeden typ włókna może być zbyt kosztowny. W niniejszym opracowaniu opisano tkaninę 3D szkło/aramid/epoksyd kompozytu hybrydowego wyprodukowanego z Kevlaru i Zylonu w kierunku Z oraz szkła w obu kierunkach X i Y. Badano właściwości mechaniczne takie jak wytrzymałość na rozciąganie, ciśnienie, trzypunktowe zginanie, odporność na uderzenie, odporność na przebicie i DMA. Kompozyty hybrydowe 3D w porównaniu z kompozytem FVF wykazują wyraźnie lepszą odporność na uderzenie, przebicie oraz właściwości DMA.